Journal of Electronic Imaging

JElectronicImaging.org

Color local binary patterns: compact descriptors for texture classification

Audrey Ledoux
Olivier Losson
Ludovic Macaire

Audrey Ledoux, Olivier Losson, Ludovic Macaire, "Color local binary patterns: compact descriptors for texture classification," *J. Electron. Imaging* **25**(6), 061404 (2016), doi: 10.1117/1.JEI.25.6.061404.

Journal of Electronic Imaging 25(6), 061404 (Nov/Dec 2016)

Color local binary patterns: compact descriptors for texture classification

Audrey Ledoux,* Olivier Losson, and Ludovic Macaire
Université de Lille, CNRS, Centrale Lille, UMR 9189 Centre de Recherche en Informatique Signal et Automatique de Lille, Bâtiment, P2, 59655 Villeneuve d'Ascq Cedex, F-59000 Lille, France

Abstract. Texture description is a challenging problem with color images. Despite some attempts to include colors in local binary patterns (LBPs), no proposal has emerged as a color counterpart of grayscale LBPs. This is because colors are defined by vectors that are not naturally ordered and several ways exist to compare them. We propose an LBP extension that takes the vector information of color into account due to a color order. As several color orders are available and the selection of the most suitable one is difficult, we combine two of them in a texture descriptor called "mixed color order LBPs." This small-size feature provides good performance on several benchmark databases for two classification problems with regard to larger-size LBP-based features of color textures. *© 2016 SPIE and IS&T* [DOI: 10.1117/1.JEI.25.6.061404]

Keywords: local binary pattern; color texture classification; color order.

Paper 16044SS received Jan. 18, 2016; accepted for publication Apr. 5, 2016; published online May 4, 2016.

1 Introduction

Color texture analysis is required in several fundamental problems of image processing such as image segmentation,[1] object recognition,[2] and texture image classification.[3] For this purpose, a texture image is described by some visual cues represented by statistical structures (e.g., histograms), hereafter called texture features. To classify the texture image, its features are compared with those of other texture samples.

As shown by several authors,[4–6] texture features that take the color information into account improve the characterization of color textures, especially when dealing with natural textures observed under fixed lighting conditions. When color images are considered, each pixel is characterized by a three-dimensional (3-D) vector whose coordinates are its red (R), green (G), and blue (B) color component levels, and several strategies have been developed to compute color texture features.[7–9]

The first and most widely used strategy is the marginal one.[10–12] It assumes that the texture can be separately described within each color component image where pixels are characterized by only one color component level. Texture features designed for grayscale images are then computed for each color component image and aggregated into a global feature representation. The other main strategy takes advantage of the color vector information. Texture features may then provide global statistics about the spatial arrangement of colors in the image plane such as the Fourier spectrum,[13] Gaussian mixture models,[14] and fractal dimension/signature.[15,16] A local analysis may also take the spatial correlation between colors of neighboring pixels into account, and provide texture features such as color co-occurrence matrices[17,18] and the histogram of local color vector patterns.[19]

Among local texture descriptors computed from grayscale images, local binary patterns (LBPs) and their variants are widely used, e.g., for face image analysis.[20,21] To compute LBPs, the gray level of each pixel is compared with those of its neighbors. The texture feature is the LBP histogram whose bin count depends on the neighborhood size. In Sec. 2, we focus on completed LBPs that have recently emerged as one of the best performers in a comprehensive comparative study of texture features.[22] The original LBP encodes the level difference sign in the neighborhood of each pixel as an integer value.[5] Guo et al.[23] complete it by the difference magnitude and show that the combined sign and magnitude improve texture classification results. Therefore, we primarily here consider their "completed LBPs" made of these terms, and call them LBPs for short.

Color texture characterization by LBPs requires the comparison of colors of neighboring pixels. As colors are defined by vectors that are not naturally ordered, there exist several ways to compare them. In Sec. 3, we detail how previous works exploit LBPs to characterize color textures. We see that the LPBs applied to color images and published so far often neglect the spatial correlation between the three color components and are more memory-consuming than grayscale LBPs.

In Sec. 4, we propose color LBPs that provide features of the same size as grayscale LBPs while taking advantage of the full color vector information. Color LBPs require the definition of a color order to compare the colors of neighboring pixels. We detail the most known color orders and show that it is not easy to determine which one provides the most discriminating texture feature for a studied database. That leads us to embed two different color orders into a descriptor called "mixed color order LBPs" (MCOLBP) (see Sec. 5). This one exploits any pair of color orders among all the available ones at no extra memory cost. In Sec. 6, we finally compare the classification performances reached by our descriptors and by other LBP-based approaches on color texture databases.

*Address all correspondence to: Audrey Ledoux, E-mail: audrey.ledoux@univ-lille1.fr

2 Local Binary Patterns

In the following sections, we recall the computation of LBPs for grayscale images and detail how their histograms are used to compare images.

2.1 *Local Binary Pattern Definition*

Let I be a grayscale image in which each pixel x is characterized by its gray level I_x. LBPs are texture descriptors that characterize the level variations in the neighborhood $\mathcal{N}_x^{P,d}$ made of P pixels at spatial distance d from x. They are made of three operators S, M, and C, expressed at each pixel as

$$\mathrm{S}[I](x) = \sum_{q \in \mathcal{N}_x^{P,d}} \mathfrak{s}(I_q, I_x) 2^{\xi(q)}, \tag{1}$$

$$\mathrm{M}[I](x) = \sum_{q \in \mathcal{N}_x^{P,d}} \mathfrak{s}(|I_q - I_x|, \mathfrak{T}_{\mathfrak{m}}) 2^{\xi(q)}, \tag{2}$$

$$\mathrm{C}[I](x) = \mathfrak{s}(I_x, \bar{\mathrm{I}}), \tag{3}$$

$$\text{with} \quad \mathfrak{s}(\alpha, \mathfrak{T}) = \begin{cases} 1 & \text{if } \alpha \geq \mathfrak{T}, \\ 0 & \text{otherwise,} \end{cases} \tag{4}$$

where $\xi(q) \in \{0, \ldots, P-1\}$ is the index of each neighbor q (whose weight is $2^{\xi(q)}$). The S operator uses the binary comparison function $\mathfrak{s}$ to characterize the inferiority/superiority of the level I_q of each neighbor q with respect to the level I_x of the central pixel x. The M operator characterizes the local level difference magnitude, and the associated threshold $\mathfrak{T}_{\mathfrak{m}}$ is chosen as the average of the local difference magnitude over the N pixels of the image ($\mathfrak{T}_{\mathfrak{m}} = \frac{1}{NP} \sum_{x \in I} \sum_{q \in \mathcal{N}_x^{P,d}} |I_q - I_x|$). The C operator is just the binarization of I_x using the average level ($\bar{\mathrm{I}} = \frac{1}{N} \sum_{x \in I} I_x$) as threshold.

Let us note that the S operator is sometimes parameterized with a threshold to provide a more noise-robust descriptor,[24] but that is out of the scope of this paper. In addition, the values of S and M operators can be represented as a P-bit image, and those of C as a binary image.

2.2 *Histogram Computation*

To compare texture images efficiently, the information carried by each LBP descriptor is summarized by the histogram of its values. The v'th histogram bin value ($v \in \{0, \ldots, 2^P - 1\}$ for S and M, and $v \in \{0, 1\}$ for C) are computed from the LBP images $\mathrm{Op}[I]$ as $H_{\mathrm{Op}}(v) = \mathrm{Card}(\{x \in I | \mathrm{Op}[I](x) = v\})$, where Op denotes any of the three LBP operators and Card is the cardinality. These operators can be used together to form new features. The C operator is only used jointly with S or/and M because H_C is a poor feature. But S and M can be merged either separately by the concatenation (symbolized by "–") of their histograms into $H_{\mathrm{S-M}} \triangleq H_{\mathrm{S}} - H_{\mathrm{M}}$, or jointly by the joint two-dimensional (2-D) histogram (symbolized by "×") computed as $H_{\mathrm{S\times M}}(\mathbf{v}) = Card(\{x \in I | (\mathrm{S}[I](x) = v_1) \wedge (\mathrm{M}[I](x) = v_2)\})$, where $\mathbf{v} = (v_1, v_2) \in \{0, \ldots, 2^P - 1\}^2$. Finally, all three LBP operators can be considered either jointly, which provides $H_{\mathrm{S\times M\times C}}$, or hybridly by the concatenation of their histograms, which provides $H_{\mathrm{S-M\times C}} \triangleq H_{\mathrm{S}} - H_{\mathrm{M,C=0}} - H_{\mathrm{M,C=1}}$ and $H_{\mathrm{M-S\times C}} \triangleq H_{\mathrm{M}} - H_{\mathrm{S,C=0}} - H_{\mathrm{S,C=1}}$.

Table 1 shows the combinations of operators (COp) whose histograms are used as texture features in this paper and the corresponding bin count. Since this size ranges between 2^P and 2^{2P+1}, it is important to consider it when assessing the texture descriptor performance in classification tasks.

2.3 *Similarity Between Two Images*

The classification process requires a similarity measure to compare images. Among the measures proposed in the literature (e.g., the Euclidean distance, Manhattan distance, and log-likelihood measure),[25] we choose to compare two images I' and I'' by the normalized intersection between their LBP histograms H'_{COp} and H''_{COp}

$$Sim_{\mathrm{COp}}(I', I'') = \frac{1}{\varsigma} \sum_v \min[H'_{\mathrm{COp}}(\mathbf{v}), H''_{\mathrm{COp}}(\mathbf{v})], \text{ with}$$
$$\varsigma = \sum_v H'_{\mathrm{COp}}(\mathbf{v}) = \sum_v H''_{\mathrm{COp}}(\mathbf{v}), \tag{5}$$

where COp denotes any of the COp described in Table 1 and v stands for either a single, a pair, or a triplet of values according to whether H' and H'' are concatenated, joint, or hybrid histograms. $Sim_{\mathrm{COp}}(I', I'')$ ranges from 0 to 1 and is close to 1 when the two images are similar.

3 Local Binary Patterns for Color Texture Description

LBP operators are based on the comparison between the levels of neighboring pixels [see Eqs. (1)–(4)]. Their extension to color images is not straightforward because colors are not naturally ordered as gray levels. Indeed, each pixel x in a RGB color image $\mathbf{I}$ is characterized by a vector of three color component values $\mathbf{I}_x = (I_x^R, I_x^G, I_x^B)$. In the context of color texture classification, most authors skirt the color order problem and use one of the three following strategies.

3.1 *Luminance Local Binary Patterns and Color Features*

Like Mäenpää and Pietikäinen,[7] Ning et al.[26] assume that the color texture is jointly described by the color distribution in the color space and by the arrangement of the luminance (that is deduced from the three color components) in the spatial image domain. The color distribution is characterized by the color histogram and the luminance arrangement is

Table 1 Histogram size for the different combinations of LBP operators (COp).

Histogram H_{COp}	Bin count
H_{S}, H_{M}	2^P
$H_{\mathrm{S-M}}$	$2^P + 2^P$
$H_{\mathrm{S\times C}}$	$2^P \times 2$
$H_{\mathrm{S\times M}}$	$2^P \times 2^P$
$H_{\mathrm{S-M\times C}}$, $H_{\mathrm{M-S\times C}}$	$2^P + 2^P \times 2$
$H_{\mathrm{S\times M\times C}}$	$2^P \times 2^P \times 2$

described by the histogram of LBPs (S operator) computed from the luminance image. The color texture feature is then the concatenation of the 3-D color histogram and the LBP histogram, whose sizes are different.

Cusano et al.[27] concatenate the luminance LBP histogram computed due to the S operator with the local color contrast (LCC) histogram. At each pixel x, the LCC is obtained by comparing its color $\mathbf{I}_x$ with the average color $\bar{\mathbf{I}}_x$ of its neighbors $(\bar{\mathbf{I}}_x = (\overline{I^R}_x, \overline{I^G}_x, \overline{I^B}_x)$ with $\overline{I^k}_x = \frac{1}{P}\sum_{q\in\mathcal{N}_x^{P,d}} I_q^k$, $\forall k \in \{R,G,B\})$. In order to obtain a color descriptor that is robust against illuminant changes, the LCC is computed as the angle between $\mathbf{I}_x$ and $\bar{\mathbf{I}}_x$,

$$\mathrm{LCC}[\mathbf{I}](x) = \arccos\left(\frac{\langle \mathbf{I}_x, \bar{\mathbf{I}}_x\rangle}{\|\mathbf{I}_x\| \cdot \|\bar{\mathbf{I}}_x\|}\right), \tag{6}$$

where $\langle\cdot,\cdot\rangle$ is the inner product and $\|\cdot\|$ is the Euclidean norm. LCC values in $[0,(\pi/4)]$ are uniformly quantized so that the LCC histogram contains 256 bins, and the few values in $[(\pi/4),(\pi/2)]$ are assigned to the last bin. The texture feature is then the concatenation of the luminance LBP and LCC histograms into $H_{\mathrm{S-LCC}} \triangleq H_{\mathrm{S}} - H_{\mathrm{LCC}}$.

Lee et al.[21] characterize a texture image by the concatenation of four LBP histograms, namely one for the color vector norm, that brings the same information as luminance, and three for the angles between the possible pairs of different color components. The angle between two components $(k_1,k_2) \in \{R,G,B\}^2$ of a color $\mathbf{I}_x$ is expressed as

$$\theta(I_x^{k_1}, I_x^{k_2}) = \arctan\left(\frac{I_x^{k_1}}{I_x^{k_2} + \gamma}\right), \tag{7}$$

where γ is a small-valued constant to avoid division by zero. Each LBP descriptor is computed with the S operator by replacing the gray levels I_q and I_x of pixels q and x in Eq. (1) by their color vector norms $\|\mathbf{I}_q\|$ and $\|\mathbf{I}_x\|$ or by their between-component angles $\theta(I_q^{k_1}, I_q^{k_2})$ and $\theta(I_x^{k_1}, I_x^{k_2})$.

3.2 *Marginal Local Binary Patterns*

One of the most used strategies consists of marginally applying LBP operators to each color component image.[5,28–31] Although this scheme is easy to implement, it computes as many LBP images as the number of components [see Fig. 1(a)]. The texture feature is then the concatenation of the three LBP histograms. This strategy has also been applied with LBP variants such as local triplet patterns.[32] Because it is marginal, it does not take the correlation between color components into account. Therefore, Connah and Finlayson[33] adapt it by computing the memory-hungry 3-D histogram from the three marginal LBP images.

3.3 *Opponent Color Local Binary Patterns*

Mäenpää et al.[34] develop the opponent color LBP (OCLBP) operators to integrate the correlation between two color components. For this purpose, they consider each pair (k_1,k_2) of color components and compare the level $I_x^{k_1}$ of each pixel x with the level $I_q^{k_2}$ of its neighbors q. However, even if the OCLBPs have been used by several authors,[7,35,36] the six OCLBP histograms still require more memory than the three marginal LBP histograms.

All the above works about color texture characterization by LBPs define features that are highly memory-consuming, and most of them do not fully take the correlation between colors of neighboring pixels into account.

4 Color Local Binary Patterns

We propose a new color LBP that takes advantage of the spatial interaction between colors of neighboring pixels while requiring no more memory than grayscale LBPs. The output of a color LBP operator applied to a color image can indeed be stored as a single-grayscale image, requiring three times less memory than the marginal approach [see Fig. 1(b)].

In the first part of this section, we extend the LBP definition to color images due to a color order that defines the inferiority/superiority between colors. Then we detail some color orders of the literature that can be used to compute color LBPs.

4.1 *Color Local Binary Pattern Definition*

LBPs are based on a binary function $\mathfrak{s}$ that compares scalar values in the case of grayscale images [see Eq. (4)]. To compare two colors, we replace $\mathfrak{s}$ by the function $\mathfrak{S}$ that is based on a color order defined on the set of all colors in the RGB color space. The color LBP operators are then expressed at each pixel $x \in \mathbf{I}$ as

$$\mathbf{S}[\mathbf{I}](x) = \sum_{q\in\mathcal{N}_x^{P,d}} \mathfrak{S}(\mathbf{I}_q, \mathbf{I}_x) 2^{\xi(q)}, \tag{8}$$

$$\mathbf{M}[\mathbf{I}](x) = \sum_{q\in\mathcal{N}_x^{P,d}} \mathfrak{s}(\|\mathbf{I}_q - \mathbf{I}_x\|, \mathfrak{T}_{\mathfrak{m}}) 2^{\xi(q)}, \tag{9}$$

$$\mathbf{C}[\mathbf{I}](x) = \mathfrak{S}(\mathbf{I}_x, \bar{\mathbf{I}}), \tag{10}$$

$$\text{with} \quad \mathfrak{S}(\mathbf{C}_1, \mathbf{C}_2) = \begin{cases} 1 & \text{if } \mathbf{C}_1 \succeq \mathbf{C}_2, \\ 0 & \text{otherwise,} \end{cases} \tag{11}$$

where $\succeq$ is the color comparison operator that is specific to the color order used. The $\mathbf{S}$ operator characterizes the inferiority/superiority between the color of the central pixel x and those of its neighbors q. The $\mathbf{M}$ operator characterizes the

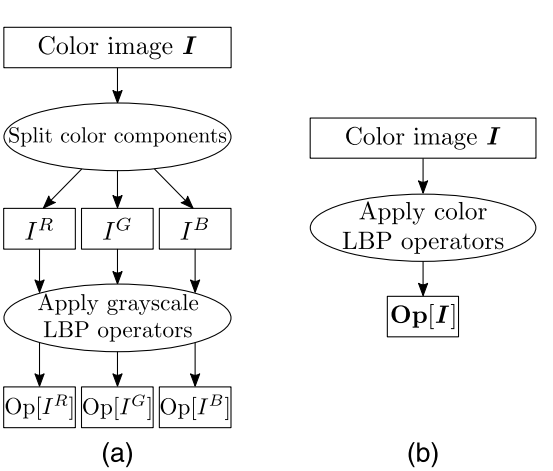

Fig. 1 LBP computation from a color image using (a) a marginal or (b) a vector strategy. Here, Op denotes either the S, M, or C operator.

local difference magnitude computed with the Euclidean color distance. The distance between the colors $\mathbf{I}_q$ and $\mathbf{I}_x$ is compared to the threshold $\mathfrak{T}_{\mathfrak{m}}$ which is the mean Euclidean color distance between each pixel and its neighbors over the whole image ($\mathfrak{T}_{\mathfrak{m}} = \frac{1}{NP}\sum_{x\in I}\sum_{q\in\mathcal{N}_x^{P,d}} \|I_q - I_x\|$). The $\mathbf{C}$ operator is similar to a thresholding; it compares $\mathbf{I}_x$ to the average color $\bar{\mathbf{I}} = (\overline{I^R}, \overline{I^G}, \overline{I^B})$ computed as $\overline{I^k} = \frac{1}{N}\sum_{x\in I} I_x^k$ for each component $k \in \{R, G, B\}$.

The $\mathbf{S}$ and $\mathbf{C}$ operators (unlike $\mathbf{M}$) use the comparison function $\mathfrak{S}$ that involves the $\succeq$ operator to compare two colors. This operator defines a binary relation that is an order[37] provided that the following statements hold for all colors $\mathbf{C}_1$, $\mathbf{C}_2$, and $\mathbf{C}_3$

$$\text{reflexivity}: \mathbf{C}_1 \succeq \mathbf{C}_1,$$

$$\text{transitivity}: (\mathbf{C}_1 \succeq \mathbf{C}_2) \wedge (\mathbf{C}_2 \succeq \mathbf{C}_3) \Rightarrow \mathbf{C}_1 \succeq \mathbf{C}_3,$$

$$\text{antisymmetry}: (\mathbf{C}_1 \succeq \mathbf{C}_2) \wedge (\mathbf{C}_2 \succeq \mathbf{C}_1) \Rightarrow \mathbf{C}_1 = \mathbf{C}_2.$$

The order is totaled when all pairs of colors are comparable ($\mathbf{C}_1 \succeq \mathbf{C}_2$ or $\mathbf{C}_2 \succeq \mathbf{C}_1$), which is a stronger condition than reflexivity. In addition, when the antisymmetry property is not met, the relation is a preorder. In the following, we detail the color relations that are the most used in the literature.[37]

4.2 *Intensity-Based Preorder*

A straightforward way to obtain an order on the color set is to reduce the color vector to its intensity (or luminance) level.[7] We compute the intensity of a color $\mathbf{C} = (C^R, C^G, C^B)$ as

$$Int(\mathbf{C}) = 0.299 \cdot C^R + 0.587 \cdot C^G + 0.114 \cdot C^B. \tag{12}$$

As several colors can have the same intensity, the intensity-based comparison does not satisfy the antisymmetry property and is a preorder defined as

$$\mathbf{C}_1 \succeq \mathbf{C}_2 \Leftrightarrow Int(\mathbf{C}_1) \geq Int(\mathbf{C}_2). \tag{13}$$

The chromaticity is lost by the intensity computation and the color LBPs based on this preorder are equivalent to the LBPs obtained from the intensity image.

4.3 *Lexicographic Order*

The lexicographic order is widely used in nonlinear multivalued image processing because it builds a total order.[38,39] It is based on priorities between the components k_j of a vector. Using the priorities $k_1 \triangleright k_2 \triangleright k_3$, where $\triangleright$ means "has priority over," a color $\mathbf{C}_1$ is considered as greater than or equal to a color $\mathbf{C}_2$ according to the rule

$$\begin{aligned}\mathbf{C}_1 \succeq \mathbf{C}_2 \Leftrightarrow\ & (C_1^{k_1} > C_2^{k_1}) \vee [(C_1^{k_1} = C_2^{k_1}) \wedge (C_1^{k_2} > C_2^{k_2})] \\ & \vee [(C_1^{k_1} = C_2^{k_1}) \wedge (C_1^{k_2} = C_2^{k_2}) \wedge (C_1^{k_3} \geq C_2^{k_3})],\end{aligned} \tag{14}$$

where $C_i^{k_j}$ denotes the component k_j, $j = 1\ldots3$, of the color $\mathbf{C}_i$. The lexicographic order induces a prioritization problem between color components. The component used first to order the colors [k_1 in Eq. (14)] is favored, which strongly affects the final result.

4.4 *Bit Mixing Order*

The "bit mixing" is a popular way to design nonlinear filters in the color domain.[40] It provides a total order by associating a different integer to each different color. This integer is obtained by mixing the bits of the three color components of any color $\mathbf{C}$ as

$$\mathfrak{N}(\mathbf{C}) = \sum_{b=1}^{L}\left\{2^{3\cdot(b-1)} \cdot \sum_{k=1}^{3} 2^{3-r_k} \cdot c^{r_k,b}\right\}, \tag{15}$$

where $r_k \in \{1, 2, 3\}$ is the rank associated to the color component $k \in \{k_1, k_2, k_3\}$ whose value C^k is represented as the L-bit sequence $\{c^{r_k,b}\}_{b=L\ldots1}$. The "bit mixing" order is then defined as

$$\mathbf{C}_1 \succeq \mathbf{C}_2 \Leftrightarrow \mathfrak{N}(\mathbf{C}_1) \geq \mathfrak{N}(\mathbf{C}_2). \tag{16}$$

The "bit mixing" induces the same prioritization problem as the lexicographic order (we have $k_1 \triangleright k_2 \triangleright k_3$ when $r_{k_1} < r_{k_2} < r_{k_3}$), even if it has less influence on the result.

4.5 *Preorder Based on the Color Vector Norm*

Several authors extend LBPs to the color and multispectral domains using the color vector norm.[19,41,42] The comparison relation is then defined as

$$\mathbf{C}_1 \succeq \mathbf{C}_2 \Leftrightarrow \|\mathbf{C}_1\| \geq \|\mathbf{C}_2\|. \tag{17}$$

This color order neglects the chromaticity of the two compared colors such as the intensity-based one. In addition, since different colors can be characterized by the same vector norm, this relation is a preorder.

4.6 *Preorder Based on a Reference Color*

This color comparison relation is based on the Euclidean distance between any color and a reference color $\mathbf{C}_{\text{ref}}$.[16] The relation that compares two colors $\mathbf{C}_1$ and $\mathbf{C}_2$ with respect to $\mathbf{C}_{\text{ref}}$ is defined as

$$\mathbf{C}_1 \succeq \mathbf{C}_2 \Leftrightarrow \|\mathbf{C}_1 - \mathbf{C}_{\text{ref}}\| \geq \|\mathbf{C}_2 - \mathbf{C}_{\text{ref}}\|. \tag{18}$$

This relation provides a preorder. As the reference color $\mathbf{C}_{\text{ref}}$ can be any color of the color space, it is the parameter of this color order. When $\mathbf{C}_{\text{ref}}$ is the black color $\mathbf{O} = (0, 0, 0)$, it is similar to the preorder based on the vector norm. We expect to improve the texture classification performance by selecting the reference color with care (see Sec. 6.2).

4.7 *Comparison of the Color Orders*

All the color orders introduced previously (see Table 2) transform the two colors to be compared into scalars and compare these scalars. As these orders differ according to their definition of the color relation, we propose to use an illustrative example to study the differences among them. In this aim, we illustrate the relation between any color $\mathbf{C}_1$ and a given color $\mathbf{C}_2$ deduced from the different color orders on a simple example restricted to R and G components coded with three bits (see Fig. 2). The color $\mathbf{C}_2$ is marked as a red diagonal cross, and the colors marked as squares are higher than or equal to $\mathbf{C}_2$ while those marked as dots are lower.

Table 2 Notations for the color orders detailed in this paper.

Color order	Equations	Notation
Intensity-based	(13)	$\mathfrak{S}^{Int}$
Lexicographic with priorities $k_1 \triangleright k_2 \triangleright k_3$	(14)	$\mathfrak{S}^{Lex}_{k_1,k_2,k_3}$
Bit mixing with priorities $k_1 \triangleright k_2 \triangleright k_3$	(16)	$\mathfrak{S}^{Mix}_{k_1,k_2,k_3}$
Color vector norm	(17)	$\mathfrak{S}^{\epsilon}_{\mathbf{O}}$
Euclidean distance with respect to reference color $\mathbf{C}_{ref}$	(18)	$\mathfrak{S}^{\epsilon}_{\mathbf{C}_{ref}}$

In Fig. 2(a), the domain where $\mathbf{C}_1 \prec \mathbf{C}_2$ using the intensity-based order is below the straight line defined by $0.299R + 0.587G = Int(\mathbf{C}_2)$. Figure 2(b) shows the lexicographic order according to the priority $R \triangleright G$. The domain where $\mathbf{C}_1 \prec \mathbf{C}_2$ according to the bit mixing [see Fig. 2(c)] is smaller than that given by the lexicographic order according to the same priority $R \triangleright G$ (equivalent to $r_R = 1$ and $r_G = 2$). According to the order based on the color norm [see Fig. 2(d)], this color domain is a quarter disk centered at $\mathbf{O} = (0,0)$ and with radius $\|\mathbf{C}_2\|$. Using the color Euclidean distance with respect to the reference color $\mathbf{C}_{\text{ref}} = (4,4)$ [marked as a gray cross on Fig. 2(e)], the color domain is a disk centered at $\mathbf{C}_{\text{ref}}$ and with radius $\|\mathbf{C}_2 - \mathbf{C}_{\text{ref}}\|$.

This simple example shows that the size and shape of the domain $\mathbf{C}_1 \prec \mathbf{C}_2$ strongly vary with respect to the color order. So, the color LBP output depends on the chosen color order.

5 Mixed Color Order Local Binary Patterns

Several color orders presented in Table 2 use parameters, e.g., priorities between color components for the lexicographic $\mathfrak{S}^{\text{Lex}}$ and bit mixing $\mathfrak{S}^{\text{Mix}}$ orders, or the reference color for $\mathfrak{S}^{\epsilon}_{C_{\text{ref}}}$. In the first part of this section, we perform a case study experiment to compare the discriminating power of color LBPs computed with different color orders and parameter sets. They show that selecting the most relevant color order for texture classification by color LBPs strongly depends on the image database. In the second part of this section, we propose a new color LBP operator that combines two different color orders among the available ones.

5.1 *Color Order and Parameter Selection*

We propose to experimentally determine the most relevant color order among those in Table 2 by discriminating the textures in a database at best, for different parameter sets of each color order. The parameter sets of $\mathfrak{S}^{\text{Lex}}$ and $\mathfrak{S}^{\text{Mix}}$ orders are the six possible component priority triplets. For the distance-based orders $\mathfrak{S}^{\epsilon}$, we use the eight vertices of the RGB color cube as reference colors for stability's sake,[38] and retain the four best, namely $\mathbf{O}$, $\mathbf{W} = (255,255,255)$, $\mathbf{G} = (0,255,0)$, and $\mathbf{M} = (255,0,255)$. As this evaluation is restricted to the color orders and their parameters, each image is characterized by the sole histogram of the $\mathbf{S}$ operator [see Eq. (8)], with $P = 8$ and $d = 2$. We use Eq. (5) to measure the similarity between two images.

The color distribution of an image depends on the illuminant used during its acquisition. To study the behavior of different color LBPs both when the illuminant changes or not, we use two reference texture datasets from the Outex database:[43] Outex_TC_00013, whose illumination is fixed, and Outex_TC_00014, for which the illuminant changes between two compared images (see details in Sec. 6.1).

The most suitable color order should provide the largest within-class similarity (images of a same class should share similar texture features) as well as the lowest between-class similarity (texture features of images that belong to different classes should be different). For a given (combination of)

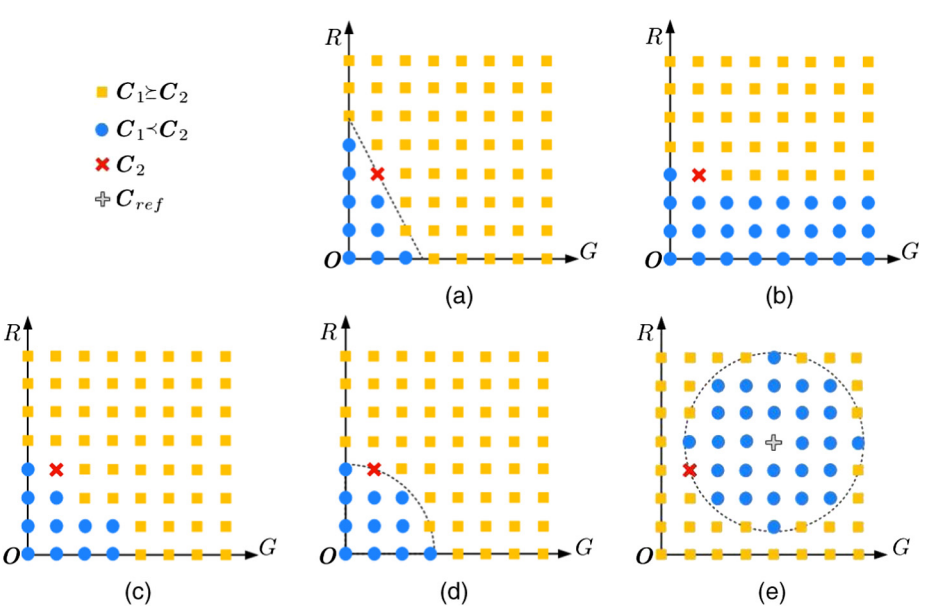

Fig. 2 Definition of the relation between any color $\mathbf{C}_1$ and a color $\mathbf{C}_2$ in the RG plane. The used color orders are (a) intensity-based $\mathfrak{S}^{Int}$, (b) lexicographic $\mathfrak{S}^{Lex}_{R,G}$, (c) bit mixing $\mathfrak{S}^{Mix}_{R,G}$, (d) based on the vector norm $\mathfrak{S}^{\epsilon}_{\mathbf{O}}$, and (e) based on the distance to a reference color $\mathfrak{S}^{\epsilon}_{(4,4)}$.

operator(s) COp and a color order associated with a parameter set, these similarities are computed as follows for each class ω_i, $i = 1 \ldots N_c$, that is represented by N_i texture samples $\mathbf{I}_s$

$$WSim_{\mathrm{COp}} = \frac{1}{N_c \cdot N_i \cdot (N_i - 1)} \cdot \sum_{i=1}^{N_c} \sum_{s=1}^{N_i} \sum_{\substack{t=1 \\ t \neq s}}^{N_i} Sim_{\mathrm{COp}}(\mathbf{I}_s, \mathbf{I}_t) \quad \text{with } \mathbf{I}_s, \mathbf{I}_t \in \omega_i, \tag{19}$$

$$BSim_{\mathrm{COp}} = \frac{1}{N_c \cdot N_i} \cdot \sum_{i=1}^{N_c} \sum_{s=1}^{N_i} \left(\frac{1}{(N_c - 1) \cdot N_j} \cdot \sum_{\substack{j=1 \\ j \neq i}}^{N_c} \sum_{t=1}^{N_j} Sim_{\mathrm{COp}}(\mathbf{I}_s, \mathbf{I}_t) \right) \begin{matrix} \text{with } \mathbf{I}_s \in \omega_i \\ \text{and } \mathbf{I}_t \in \omega_j \end{matrix}, \tag{20}$$

where Sim_{COp} is defined by Eq. (5). Table 3 only shows the four color orders and parameter sets that provide the largest within-class similarity or the smallest between-class similarity (written as bold) for at least one dataset. As we can see, the most relevant color order differs according to the between-class/within-class similarity and the dataset. Moreover, within-class and between-class similarities are close whatever the color order and parameter sets.

This experiment shows that it is difficult to identify which color order provides the best discriminating power of color LBPs. Hence, we propose a new descriptor, called "MCOLBP" and detailed in the following, that combines two orders without increasing the feature size.

5.2 *Mixed Color Order Local Binary Pattern Definition*

The MCOLBP is deduced from the "orthogonal combination" of LBPs by Zhu et al.[31] that splits the neighborhood of each pixel into two nonoverlapping subsets. Let us consider a pixel x and denote as q_i, $i = 0, \ldots, P-1$, each of its P neighbors uniformly located at spatial Euclidean distance d around x such that $\xi(q_i) = i$. The neighborhood $\mathcal{N}_x^{P,d}$ of x is split into two subsets of $P/2$ pixels (see Fig. 3): $\mathcal{N}_x^{P,d,0} = \{q_i \in \mathcal{N}_x^{P,d} | i \bmod 2 = 0\}$ and $\mathcal{N}_x^{P,d,1} = \{q_i \in \mathcal{N}_x^{P,d} | i \bmod 2 = 1\}$, where mod is the modulo operator.

We orthogonally combine different color LBPs by associating a specific color order to each neighborhood subset. The color of x is compared with those of the pixels in $\mathcal{N}_x^{P,d,0}$ due to a color order denoted as $\mathfrak{S}^0$ and with those of the pixels in $\mathcal{N}_x^{P,d,1}$ due to another color order $\mathfrak{S}^1$. This strategy can be only applied to the **S** operator because **M** does not require any color order and **C** only compares two colors.

The modified **S** operator of the MCOLBP is denoted as $\ddot{\mathbf{S}}$ and defined due to the index i of the P neighbors q_i as

$$\ddot{\mathbf{S}}[\mathbf{I}](x) = \sum_{i=0}^{P-1} \mathfrak{S}^{i \bmod 2}(\mathbf{I}_{q_i}, \mathbf{I}_x) 2^i, \tag{21}$$

where $\mathfrak{S}^0$ and $\mathfrak{S}^1$ are two of the color orders described in Table 2. Since $\ddot{\mathbf{S}}$ values range between 0 and $2^P - 1$, the bin count of its histogram is 2^P, like that of the grayscale LBP operator S.

Table 3 Within-class ($WSim_{\mathbf{S}}$) and between-class ($BSim_{\mathbf{S}}$) similarities [see Eqs. (19) and (20)] of the four best color orders and their parameter sets using the **S** operator on two Outex datasets [$N_c = 68$ classes, $N_i = 20$ (Outex_TC_00013) or $N_i = 30$ (Outex_TC_00014) samples in each class ω_i].

	Outex_TC_00013		Outex_TC_00014	
Color order	$WSim_{\mathbf{S}}$	$BSim_{\mathbf{S}}$	$WSim_{\mathbf{S}}$	v
$\mathfrak{S}^{Int}$	0.9183	**0.7069**	0.8990	0.7086
$\mathfrak{S}^{Mix}_{G,R,B}$	0.9165	0.7166	**0.9023**	0.7146
$\mathfrak{S}^{\epsilon}_{\mathbf{O}}$	0.9154	0.7070	0.8945	**0.7084**
$\mathfrak{S}^{\epsilon}_{\mathbf{G}}$	**0.9282**	0.7483	0.8917	0.7556

6 Texture Classification

To compare the discriminating power of the considered color LBPs, we perform color texture classification due to a supervised learning scheme. As is usually done to assess new features, we group samples of each texture class into the train and test subsets according to the hold-out strategy. We also retain the 1-NN classifier coupled with the similarity measure based on LBP histograms (see Sec. 2.3) since this classification scheme requires no parameter.

Since we focus on the relation order between colors in this paper, we have to use experimental datasets[44] in which train and test images represent the same textures and only differ in color distribution. This leads us to consider datasets with identical acquisition conditions for the train and test subsets, except the illuminant (see Sec. 6.1). Section 6.2 presents the classification results obtained by color LBPs applied to these datasets. Then the classification performance of MCOLBPs is assessed and discussed. Finally, since rotation-invariant uniform LBPs[45] are widely used in many applications due to their good results in retrieval tasks, we study how color LBPs and MCOLBPs can be made robust against in-plane rotations of textures. Note that all these results have been obtained using the RGB color space (the L*a*b* and HSL color spaces provided lower classification rates).

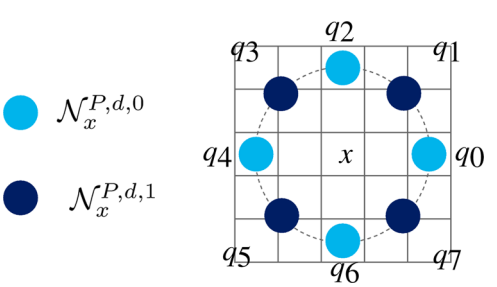

Fig. 3 Spatial locations of the neighbors q_i of a pixel x according to their membership to $\mathcal{N}_x^{P,d,0}$ or $\mathcal{N}_x^{P,d,1}$ subset (for $P = 8$ and $d = 2$).

6.1 *Texture Datasets*

To assess both the discriminating power of color LBPs and their robustness against illuminant changes, we use benchmark datasets in which train and test images have been acquired in either strictly identical conditions (under the same illuminant) or under different illuminants.

6.1.1 *Datasets with identical acquisition conditions*

First, we focus on the ability of color LBPs to discriminate textures captured in the same acquisition conditions. In this aim, we use Outex_TC_00013,[43] Barktex,[46] and USPtex[15] datasets, in which the train and test subsets contain half of the samples of each class.

Outex_TC_00013 contains texture images acquired by a three-CCD color camera under the same controlled conditions (100 dpi resolution, 0 deg rotation, and incandescent lamp at 2856 K as lighting). This dataset is made up of 68 classes, each containing 10 samples of size 128×128 pixels.[17]

Barktex is a dataset of tree bark images acquired under natural (daylight) illumination conditions. We use the modified version of Barktex built by Porebski et al.[47] from regions of interest of the original images that focus on the bark and exclude the background from texture analysis. This dataset is made up of six classes, each containing 272 samples of size 64×64 pixels.

USPtex contains 2292 images of natural textures acquired under an unknown but fixed light source. This dataset is made up of 191 classes, each containing 12 samples of size 128×128 pixels.

6.1.2 *Datasets with varying illuminant*

Our color LBPs are based on the comparison between colors of neighboring pixels. However, colors strongly depend on the spectral power distribution of the illuminant used during the image acquisition.[48] So, a given texture observed under different illuminants yields different color texture images. We, therefore, propose to study the ability of color LBPs to discriminate textures viewed under different illuminants using Outex_TC_00014[43] and four datasets built from the Amsterdam Library of Textures[3] (ALOT).

The train images of Outex_TC_00014 are the same as Outex_TC_00013. The test subset of each class contains 10 samples acquired under a 2300 K horizon sunlight source and 10 samples acquired under a TL84 4000 K fluorescent light source.

We also use four datasets built from the ALOT database and called ALOT_ill_c1–c4 (available from Ref. 49). All images in a dataset that represent the original 250 classes have a size of 768×512 pixels, and have been acquired from the same viewpoint given by a camera $(c1, \ldots, c4)$ under either a 3075 K illuminant (1 train image by class) or a 2175 K illuminant (one test image by class).

6.2 *Classification Results of Color Local Binary Patternss*

Here we aim to show the contribution of the color order used to compute color LBPs for texture classification purposes. Among the three operators presented in Sec. 4.1, only **S** and **C** are based on the function $\mathfrak{S}$ which uses a color order. Therefore, we present classification results using H_{S} and $H_{\mathbf{S}\times\mathbf{C}}$ histograms only. As previously mentioned, the number P of neighbors is set to 8 and the distance d between each pixel and its neighbors is set to 2 ($d = 1$ and $d = 4$ provided lower classification accuracies). Table 4(a) shows the accuracies obtained by our color LBP operator coupled with four different color orders. As parameter sets, we have retained the three best priority triplets for $\mathfrak{S}^{\mathrm{Lex}}$ and $\mathfrak{S}^{\mathrm{Mix}}$, and the four best reference colors for $\mathfrak{S}^{\epsilon}$. To compare with the other color methods described in Sec. 3, Table 4b shows the performances reached by the approaches of Lee et al.[21] based on three color angles and the color vector norm (see Sec. 3.1), Pietikäinen et al.[5] computing three marginal LBPs (see Sec. 3.2), Mäenpää et al.[34] based on six OCLBPs (see Sec. 3.3), and Cusano et al.[27] using the LCC and the luminance LBP (see Sec. 3.1).

6.2.1 *Results with identical acquisition conditions*

The middle part of Table 4(a)shows that the color order providing the best result (written as bold for each column) varies according to the feature ($H_{\mathbf{S}}$ or $H_{\mathbf{S}\times\mathbf{C}}$) and to the dataset. In detail, the best performing color LBPs rely not only on the color distance-based preorder $\mathfrak{S}^{\epsilon}_{\mathbf{G}}$ for Outex_TC_00013, but also on the color distance-based preorder $\mathfrak{S}^{\epsilon}_{\mathbf{W}}$ and the intensity-based preorder for Barktex and USPtex. So it is difficult to retain the best discriminating color order in case of a fixed illuminant.

The middle part of Table 4(b)shows that the marginal strategy[5] and OCLBPs[34] always obtain better classification accuracies than color LBPs. The approach based on color angles[21] outperforms color LBPs only for the H_{S} feature. However, the feature size required by these strategies is from three to six times larger than those required by our color LBPs. For this classification problem, LBPs based on the LCC[27] almost always provide lower classification accuracies than color LBPs with the same feature size (that of $H_{\mathrm{S}\times\mathrm{C}}$) whatever the color order used.

6.2.2 *Results with varying illuminant*

The right part of Table 4 shows the classification accuracies obtained on datasets with varying illuminants. Since results obtained with the four ALOT datasets (ALOT_ill_c1–c4) are very similar, we report their average. The best classification accuracy of color LBPs is obtained using the distance-based color order $\mathfrak{S}^{\epsilon}_{\mathbf{O}}$ with $H_{\mathbf{S}\times\mathbf{C}}$. The intensity-based order $\mathfrak{S}^{Int}$ provides close results, which confirms that it is actually similar to $\mathfrak{S}^{\epsilon}_{\mathbf{O}}$. Even more than in the previous classification problem, combining the **S** operator with **C** generally improves the accuracy (by up to 15% here).

By comparing Tables 4(a) and 4(b), we deduce that the best color LBPs outperform the four cited approaches for this problem, while requiring less memory. We conclude that taking the full color information into account is a relevant strategy in case of illuminant variations.

6.2.3 *Discussion*

As from Table 3, we can deduce from Table 4 that the best color order depends on the dataset and on the illuminant. But color orders that neglect the chromaticity like $\mathfrak{S}^{Int}$ and $\mathfrak{S}^{\epsilon}_{\mathbf{O}}$ provide the best results in six columns among the 10 ones of Table 4. These results point out that chromaticity is of little interest for texture classification. Furthermore, even if $\mathfrak{S}^{\epsilon}_{\mathbf{O}}$

Table 4 Classification accuracy (%) of the tested approaches for two kinds of classification problems: identical acquisition conditions (middle: Outex TC_00013, Barktex, USPtex), and varying illuminant (right: Outex TC_00014, ALOT ill_c1–c4), (a) color LBPs and (b) literature LBP-based methods.

(a) Color LBPs

	Feature size		Outex TC_00013		Barktex		USPtex		Outex TC_00014		ALOT ill_c1–c4	
Feature	$H_{\mathbf{S}}$	$H_{\mathbf{S\times C}}$	$H_{\mathbf{S}}$	$H_{\mathbf{S\times C}}$	$H_{\mathbf{S}}$	$H_{\mathbf{S\times C}}$	$H_{\mathbf{S}}$	$H_{\mathbf{S\times C}}$	$H_{\mathbf{S}}$	$H_{\mathbf{S\times C}}$	$H_{\mathbf{S}}$	$H_{\mathbf{S\times C}}$
Color order												
$\mathfrak{S}^{Int}$	2^P	$2^P\times 2$	81.2	84.9	**74.3**	75.3	**79.9**	83.3	**70.4**	73.9	**92.0**	96.4
$\mathfrak{S}^{Lex}_{G,R,B}$	2^P	$2^P\times 2$	82.8	85.4	72.8	74.4	78.7	83.3	69.1	73.4	90.6	95.9
$\mathfrak{S}^{Lex}_{G,B,R}$	2^P	$2^P\times 2$	82.2	86.3	73.4	75.5	79.6	84.0	65.6	72.3	89.9	96.5
$\mathfrak{S}^{Lex}_{B,R,G}$	2^P	$2^P\times 2$	82.1	85.4	70.0	74.5	77.3	80.1	47.1	52.4	40.3	53.7
$\mathfrak{S}^{Mix}_{R,G,B}$	2^P	$2^P\times 2$	81.0	85.7	70.7	75.4	77.8	79.8	65.4	67.2	82.1	80.7
$\mathfrak{S}^{Mix}_{R,B,G}$	2^P	$2^P\times 2$	83.2	85.2	72.2	75.0	78.2	79.6	65.0	66.2	79.5	77.9
$\mathfrak{S}^{Mix}_{B,R,G}$	2^P	$2^P\times 2$	81.5	84.6	72.3	74.5	79.1	79.1	62.5	64.9	72.1	72.3
$\mathfrak{S}^{\epsilon}_{\mathbf{O}}$	2^P	$2^P\times 2$	81.2	85.3	73.8	75.6	78.8	83.8	68.8	**74.3**	91.0	**97.9**
$\mathfrak{S}^{\epsilon}_{\mathbf{W}}$	2^P	$2^P\times 2$	79.6	85.9	73.9	**77.7**	78.8	**84.2**	64.0	72.3	63.4	78.5
$\mathfrak{S}^{\epsilon}_{\mathbf{G}}$	2^P	$2^P\times 2$	**83.8**	**87.1**	62.6	66.4	74.2	78.4	54.3	57.4	62.2	75.9
$\mathfrak{S}^{\epsilon}_{\mathbf{M}}$	2^P	$2^P\times 2$	82.5	85.4	72.8	73.8	66.0	69.9	63.8	69.3	28.7	24.8

(b) Literature LBP-based methods

Approach feature	H_{S}	$H_{\mathrm{S\times C}}$	H_{S}	$H_{\mathrm{S\times C}}$	H_{S}	$H_{\mathrm{S\times C}}$	H_{S}	$H_{\mathrm{S\times C}}$	H_{S}	$H_{\mathrm{S\times C}}$	H_{S}	$H_{\mathrm{S\times C}}$
Color angles[21]	4×2^P	$4\times 2^P\times 2$	86.2	85.3	80.2	74.5	88.8	79.1	66.3	73.6	49.1	97.2
Marginal[5]	3×2^P	$3\times 2^P\times 2$	86.8	89.1	76.4	79.4	85.8	89.4	65.9	72.1	89.5	96.6
OCLBPs[34]	6×2^P	$6\times 2^P\times 2$	92.5	92.2	74.6	79.4	90.8	91.9	15.7	21.8	39.1	50.0
Feature approach	$H_{\mathrm{S-LCC}}$		$H_{\mathrm{S-LCC}}$		$H_{\mathrm{S-LCC}}$		$H_{\mathrm{S-LCC}}$		$H_{\mathrm{S-LCC}}$		$H_{\mathrm{S-LCC}}$	
LCC[27]	$2^P\times 2$		82.8		71.0		80.4		71.9		47.8	

performs quite well in all cases, it is difficult to identify one color order-based LBP that reaches the best classification rates whatever the operator and classification problem. That leads us to examine the performance reached by MCOLBPs that combine two color orders.

6.3 *Classification Results of Mixed Color Order Local Binary Patterns*

Since MCOLBPs only use the $\ddot{\mathbf{S}}$ operator (see Sec. 5.2), we assess their classification results using the sole $H_{\ddot{\mathbf{S}}}$ histogram whose size is 2^P, still with $P=8$ and $d=2$. To compute MCOLBPs, we use the 11 color orders presented in Table 4(a) and we combine them orthogonally with each other. To compute one MCOLBP, each color order is used as $\mathfrak{S}^0$ and one of the 10 others as $\mathfrak{S}^1$, or conversely. So one color order is associated with 20 different MCOLBP combinations. Figures 4 and 5 show the classification accuracies of MCOLBPs versus color LBPs. For each color order on these figures, the black square shows the average result over the 20 MCOLBP combinations and the error bar shows the minimal–maximal result range. The hatched box reports the accuracy of H_S from Table 4(a) to provide a comparison with the color LBP that uses this order in the whole neighborhood. For example, the first box in Fig. 4 corresponds to the color order $\mathfrak{S}^{Int}$. The first black square and error bar show that the average, minimal, and maximal accuracies reach 82.2%, 78.1%, and 88.5%, respectively. The hatched box indicated that H_{S} computed with $\mathfrak{S}^{Int}$ provides 81.2% of well-classified images for Outex_TC_00013 dataset.

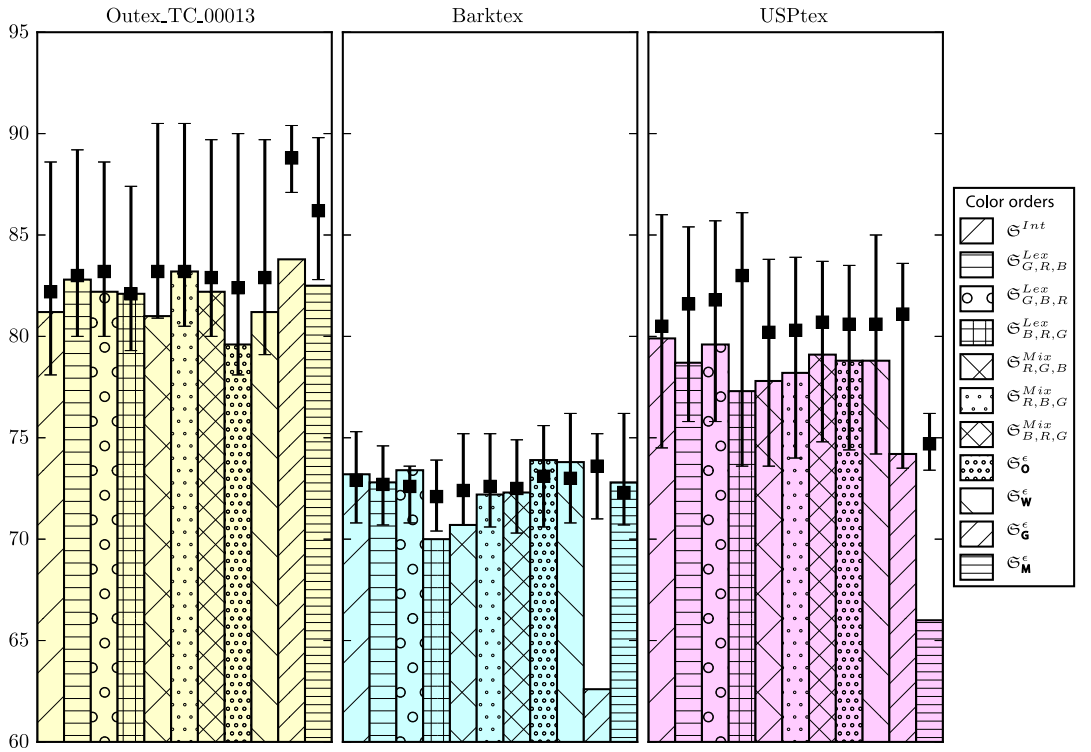

Fig. 4 Classification accuracies (%) of MCOLBPs (black squares) versus color LBPs (hatched boxes) with textures acquired in identical conditions.

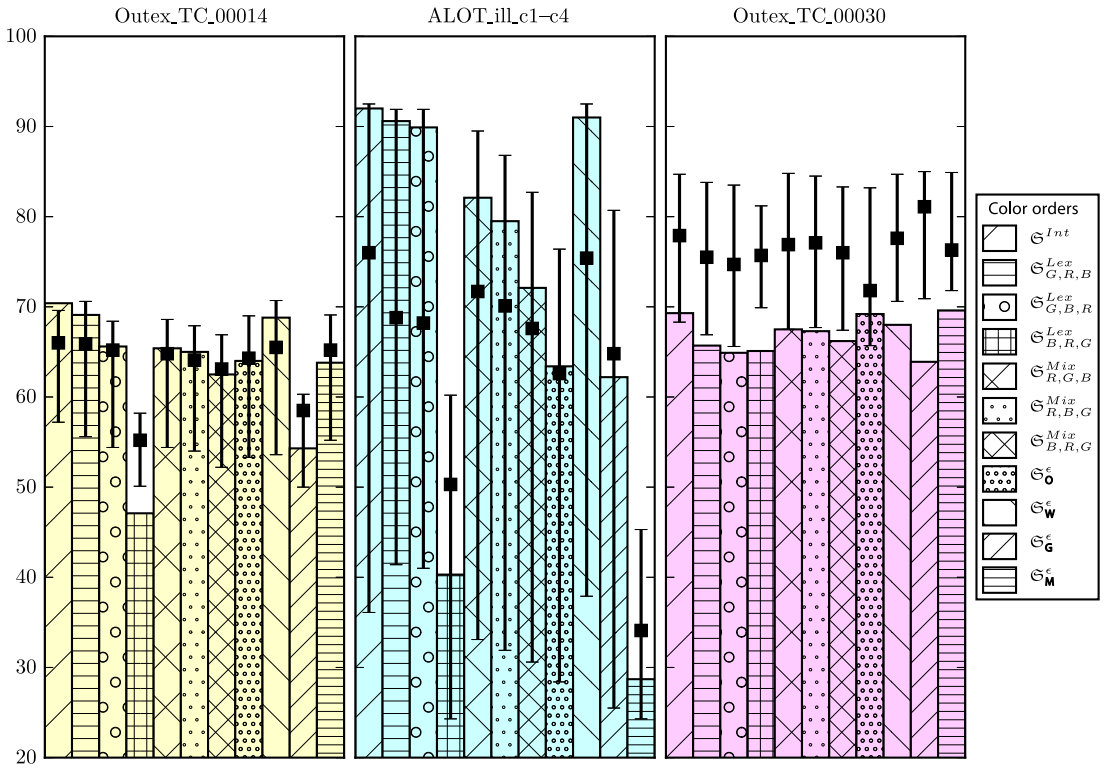

Fig. 5 Classification accuracies (%) of MCOLBPs (black squares) versus color LBPs (hatched boxes) with textures acquired under a varying illuminant (left two plots) or different rotation angles (right plot). The latter plot uses rotation-invariant descriptors MCOLBP^{riu2} and color LBP^{riu2} (see Sec. 6.4).

6.3.1 *Results with identical acquisition conditions*

Figure 4 shows that the average classification accuracy using MCOLBPs is always better than that of color LBPs on Outex_TC_00013 and USPtex, and the results are comparable on Barktex. For the three datasets, the maximal classification accuracy obtained by MCOLBPs is significantly higher than that of color LBPs. These experiments show that combining two color orders is a relevant approach when illumination conditions do not change.

By comparing Fig. 4 and Table 4(b), we see that methods in the literature generally obtain better classification accuracies than MCOLBPs but at the expense of two to six times larger memory requirements. MCOLBPs using the color order $\mathfrak{S}^{\epsilon}_{\mathbf{G}}$ may provide a very good trade-off between feature compactness and texture description power.

6.3.2 *Results with varying illuminant*

Figure 5 shows that on Outex_TC_00014, MCOLBPs provide close classification accuracy to that of color LBPs for five color orders. The classification accuracies using color LBPs or MCOLBPs strongly depend on the color order on ALOT_ill_c1–c4 datasets. For this classification problem, the maximal accuracy provided by MCOLBPs is higher than that provided by color LBPs in all but one case ($\mathfrak{S}^{Int}$). Comparison with the literature approaches yields the same conclusion as in Sec. 6.2.3; MCOLBPs based on at least one color order that neglects the chromaticity ($\mathfrak{S}^{Int}$, $\mathfrak{S}^{\epsilon}_{\mathbf{O}}$) obtain better classification accuracies than literature approaches. Indeed, illuminant variations modify texture colors as well as LBP descriptors based on a color order (see Sec. 6.1.2). The achromatic information is then the least affected, which explains why the intensity- and distance-based color orders $\mathfrak{S}^{Int}$ and $\mathfrak{S}^{\epsilon}_{\mathbf{O}}$ provide the best classification accuracies.

We can deduce from all previous results that the MCOLBP is a relevant approach in comparison to color LBPs when illumination conditions do not change. In case of varying illuminant, however, using color LBPs with a carefully chosen color order would be preferable to outperform MCOLBPs or literature LBP-based methods. The best accuracy on Outex_TC_00014 is 74.3% (see Table 4a), which is close to 76.1% obtained by Cusano et al.[27] with a feature approximately three times larger. These modest accuracies anyway confirm the conclusions of a recent study by the same authors; texture classification in case of varying illuminant is a challenging problem.[50]

6.4 *Robustness Against In-Plane Rotations*

Rotation-invariant uniform LBPs (superscripted as $riu2$)[45] are widely used in many applications due to their good results in retrieval tasks. In this last experimental part, we therefore study how color LBPs and MCOLBPs can be made robust against in-plane rotations.

Following Ojala et al.'s proposal,[45] we deduce a rotation-invariant uniform color LBP operator

$$\mathbf{S}^{riu2}[\mathbf{I}](x) = \begin{cases} \sum_{i=0}^{P-1} \mathfrak{S}(\mathbf{I}_{q_i}, \mathbf{I}_x) & \text{if } U[\mathbf{I}](x) \leq 2, \\ P+1 & \text{otherwise,} \end{cases} \tag{22}$$

where the uniformity measure $U[\mathbf{I}](x) = \sum_{i=0}^{P-1} |\mathfrak{S}(\mathbf{I}_{q_i}, \mathbf{I}_x) - \mathfrak{S}(\mathbf{I}_{q_{(i+1) \bmod P}}, \mathbf{I}_x)|$ characterizes the number of 0/1 and 1/0 bitwise transitions in the circular color LBP code at x (see Fig. 3 for the indices i of neighboring pixels q_i).

In the same way, we propose a rotation-invariant uniform MCOLBP operator $\ddot{\mathbf{S}}^{riu2}$ that relies on the two nonoverlapping neighborhood subsets $\mathcal{N}_x^{P,d,0}$ and $\mathcal{N}_x^{P,d,1}$ to use a different color order $\mathfrak{S}^0$ and $\mathfrak{S}^1$ in each of them. As shown in Fig. 3, neighboring pixels that belong to a given subset are not consecutive in $\mathcal{N}_x^{P,d}$, such that their bits are not consecutive in the circular LBP code. Furthermore, as seen in Sec. 6.2, the different color orders have different behaviors. The above uniformity measure hence cannot be used to compute $\ddot{\mathbf{S}}^{riu2}$. We propose instead to consider the uniformity inside each subset using specific measures $U^n[\mathbf{I}](x) = \sum_{\substack{i=0 \\ i \bmod 2 = n}}^{P-1} |\mathfrak{S}^n(\mathbf{I}_{q_i}, \mathbf{I}_x) - \mathfrak{S}^n(\mathbf{I}_{q_{(i+2) \bmod P}}, \mathbf{I}_x)|$, $n \in \{0, 1\}$, and to sum them up to characterize the overall uniformity of $\ddot{\mathbf{S}}^{riu2}$ at x

$$\ddot{\mathbf{S}}^{riu2}[\mathbf{I}](x) = \begin{cases} \sum_{i=0}^{P-1} \mathfrak{S}^{i \bmod 2}(\mathbf{I}_{q_i}, \mathbf{I}_x) & \text{if } U^0[\mathbf{I}](x) + U^1[\mathbf{I}](x) \leq 2, \\ P+1 & \text{otherwise.} \end{cases} \tag{23}$$

To assess our color descriptors against rotation variations, we use a dataset built from the Outex database and called Outex_TC_00030 (available from Ref. 51). Each of the 68 classes in this dataset contains 20 train images acquired in the same conditions as those of Outex_TC_00013 and 160 test images acquired using different rotation angles (5, 10, 15, 30, 45, 60, 75, and 90 deg).

The right plot in Fig. 5 shows that the classification accuracy of MCOLBPs^{riu2} (averaged over the 20 possible order combinations) is higher than that of color LBPs^{riu2} for all color orders. Moreover, this even holds for the minimal classification accuracy of MCOLBP^{riu2} for most orders (except $\mathfrak{S}^{Int}$ and $\mathfrak{S}^{\epsilon}_{\mathbf{O}}$). We conclude that the orthogonal combination of color orders embedded in MCOLBPs offers a marked advantage over color LBPs with regard to in-plane rotation robustness, and that MCOLBPs^{riu2} are fairly robust to even small rotation variations despite the doubled angular step ($4\pi/P$) between two consecutive neighbors q_i and q_{i+2} in their subset $\mathcal{N}_x^{P,d,0}$ or $\mathcal{N}_x^{P,d,1}$.

7 Conclusion

In this paper, we propose color LBPs that rely on a color order to take the full vector information of color into account unlike most of the approaches in the literature. This proposal takes advantage of the spatial interaction between colors of neighboring pixels at the same memory cost as grayscale LBPs. The output of a color LBP operator applied to a color image requires at least three times less memory than the marginal approaches. To take advantage of the properties provided by the available color orders without increasing the feature size, we combine two color orders into a single LBP operator called MCOLBP.

In the case of constant acquisition conditions, classification results confirm that it is difficult to choose a suitable color order with its parameter set because classification accuracies obtained by color LBPs are very close and the best color order is dataset-dependent. We then show that MCOLBPs improve the classification accuracy with regard to color LBPs in a great majority of the tested cases.

In the case of a varying illuminant, experiments show that color LBPs and MCOLBPs outperform approaches in the

literature when the color orders are carefully chosen. They also confirm that chromaticity is of little interest in comparison with the luminance of a color for LBP-based texture classification, and that texture classification remains an open problem in the case of a varying illuminant. Because classical methods of texture analysis tend to fail in this case, it would be interesting to generalize state-of-art methods[52–54] to color images.

We are presently working on a selection method of the best color order for a given texture classification problem. As our rotation-invariant MCOLBP operator obtains promising results, we will also study how to adapt other LBP-based descriptors among the many literature proposals to characterize color textures.

References

1. L. Shi and B. Funt, "Quaternion color texture segmentation," *Comput. Vision Image Understanding* **107**, 88–96 (2007).
2. U. Jayaraman, S. Prakash, and P. Gupta, "An efficient color and texture based iris image retrieval technique," *Expert Syst. Appl.* **39**, 4915–4926 (2012).
3. G. J. Burghouts and J.-M. Geusebroek, "Material-specific adaptation of color invariant features," *Pattern Recognit. Lett.* **30**(3), 306–313 (2009).
4. A. Drimbarean and P. F. Whelan, "Experiments in colour texture analysis," *Pattern Recognit. Lett.* **22**, 1161–1167 (2001).
5. M. Pietikäinen, T. Mäenpää, and J. Viertola, "Color texture classification with color histograms and local binary patterns," in *Proc. of the 2nd Int. Workshop on Texture Analysis and Synthesis (TEXTURE '02)*, Copenhagen, Denmark, pp. 109–112 (2002).
6. C. Palm, "Color texture classification by integrative co-occurrence matrices," *Pattern Recognit.* **37**, 965–976 (2004).
7. T. Mäenpää and M. Pietikäinen, "Classification with color and texture: jointly or separately?" *Pattern Recognit.* **37**, 1629–1640 (2004).
8. F. Bianconi et al., "Robust color texture features based on ranklets and discrete Fourier transform," *J. Electron. Imaging* **18**(4), 043012 (2009).
9. F. Bianconi et al., "Theoretical and experimental comparison of different approaches for color texture classification," *J. Electron. Imaging* **20**(4), 043006 (2011).
10. A. Bhuiyan et al., "Blood vessel segmentation from color retinal images using unsupervised texture classification," in *Proc. of the 14th IEEE Int. Conf. on Image Processing (ICIP '07)*, San Antonio, Texas, Vol. **5**, pp. 521–524 (2007).
11. J. B. Florindo and O. M. Bruno, "Fourier fractal descriptors for colored texture analysis," *Lect. Notes Comput. Sci.* **6915**, 284–292 (2011).
12. D. M. Chu and A. W. M. Smeulders, "Color invariant SURF in discriminative object tracking," *Lect. Notes Comput. Sci.* **6554**, 62–75 (2010).
13. B. Sathyabama et al., "Rotation invariant features for color texture classification and retrieval under varying illumination," *Pattern Anal. Appl.* **16**, 69–81 (2013).
14. I.-U.-H. Qazi et al., "A multivariate gaussian mixture model of linear prediction error for colour texture segmentation," in *Proc. of the 17th European Signal Processing Conf. (EUSIPCO'09)*, Glasgow, Scotland, pp. 1537–1541 (2009).
15. A. R. Backes, D. Casanova, and O. M. Bruno, "Color texture analysis based on fractal descriptors," *Pattern Recognit.* **45**, 1984–1992 (2012).
16. A. Ledoux et al., "Toward a complete inclusion of the vector information in morphological computation of texture features for color images," *Lect. Notes Comput. Sci.* **8509**, 222–229 (2014).
17. V. Arvis et al., "Generalization of the cooccurrence matrix for colour images: application to colour texture classification," *Image Anal. Stereol.* **23**, 63–72 (2004).
18. A. Porebski, N. Vandenbroucke, and L. Macaire, "Iterative feature selection for color texture classification," in *Proc. of the 14th IEEE Int. Conf. on Image Processing (ICIP '07)*, San Antonio, Texas, Vol. **3**, pp. 509–512 (2007).
19. M. Häfner et al., "Color treatment in endoscopic image classification using multi-scale local color vector patterns," *Med. Image Anal.* **16**, 75–86 (2012).
20. D. Huang et al., "Local binary patterns and its application to facial image analysis: a survey," *IEEE Trans. Syst. Man Cybern. Part C* **41**, 765–781 (2011).
21. S. H. Lee et al., "Local color vector binary patterns from multichannel face images for face recognition," *IEEE Trans. Image Process.* **21**, 2347–2353 (2012).
22. A. Fernández, M. X. Álvarez, and F. Bianconi, "Texture description through histograms of equivalent patterns," *J. Math. Imaging Vision* **45**, 76–102 (2013).
23. Z. Guo, L. Zhang, and D. Zhang, "A completed modeling of local binary pattern operator for texture classification," *IEEE Trans. Image Process.* **19**, 1657–1663 (2010).
24. M. Heikkilä and M. Pietikäinen, "A texture-based method for modeling the background and detecting moving objects," *IEEE Trans. Pattern Anal. Mach. Intell.* **28**, 657–662 (2006).
25. Y. Rubner et al., "Empirical evaluation of dissimilarity measures for color and texture," *Comput. Vision Image Understanding* **84**, 25–43 (2001).
26. J. Ning et al., "Robust object tracking using joint color-texture histogram," *Pattern Recogn. Artif. Intell.* **23**, 1245–1263 (2009).
27. C. Cusano, P. Napoletano, and R. Schettini, "Combining local binary patterns and local color contrast for texture classification under varying illumination," *J. Opt. Soc. Am. A* **31**, 1453–1461 (2014).
28. G. Han and C. Zhao, "A scene images classification method based on local binary patterns and nearest-neighbor classifier," in *Proc. of the 8th Int. Conf. on Intelligent Systems Design and Applications (ISDA '08)*, Kaohsiung, Taiwan, Vol. **1**, pp. 100–104 (2008).
29. J. Y. Choi, K. N. Plataniotis, and Y. M. Ro, "Using colour local binary pattern features for face recognition," in *Proc. of the 17th IEEE Int. Conf. on Image Processing (ICIP '10)*, Hong Kong, China, 4541–4544 (2010).
30. S. Banerji, A. Verma, and C. Liu, "LBP and color descriptors for image classification," in *Cross Disciplinary Biometric Systems*, C. Liu and V. K. Mago, eds., Intelligent Systems Reference Library, pp. 205–225, Springer, Berlin Heidelberg (2012).
31. C. Zhu, C.-E. Bichot, and L. Chen, "Image region description using orthogonal combination of local binary patterns enhanced with color information," *Pattern Recognit.* **46**(7), 1949–1963 (2013).
32. D. He and N. Cercone, "Local triplet pattern for content-based image retrieval," in *Proc. of the Int. Conf. on Image Analysis and Recognition (ICIAR '09)*, Halifax, Canada, pp. 229–238, Springer, Berlin-Heidelberg, (2009).
33. D. Connah and G. D. Finlayson, "Using local binary pattern operators for colour constant image indexing," in *Proc. of the 3rd European Conf. on Colour in Graphics, Image and Vision (CGIV '06)*, Leeds, UK, Vol. **3**, pp. 60–64 (2006).
34. T. Mäenpää, M. Pietikäinen, and J. Viertola, "Separating color and pattern information for color texture discrimination," in *Proc. of the 16th Int. Conf. on Pattern Recognition (ICPR '02)*, Québec, Canada, Vol. **1**, pp. 668–671, (2002).
35. C.-H. Chan, J. Kittler, and K. Messer, "Multispectral local binary pattern histogram for component-based color face verification," in *Proc. of the First IEEE Int. Conf. on Biometrics: Theory, Applications, and Systems (BTAS '07)*, Washington DC, pp. 1–7 (2007).
36. M. Pavithra and G. Ilanchezhiapandian, "Simulation of cancer cells growth by recognizing texture characteristics using opponent color local binary pattern," *Int. J. Comput. Sci. Mobile Comput.* **4**, 650–656 (2015).
37. V. Barnett, "The ordering of multivariate data," *J. R. Stat. Soc. A* **139**(3), 318–355 (1976).
38. E. Aptoula and S. Lefèvre, "A comparative study on multivariate mathematical morphology," *Pattern Recognit.* **40**, 2914–2929 (2007).
39. V. Barra, "Expanding the local binary pattern to multispectral images using total orderings," in *Computer Vision, Imaging and Computer Graphics. Theory and Applications*, P. Richard and J. Braz, eds., Communications in Computer and Information Science, Vol. **229**, pp. 67–80, Springer (2011).
40. J. Chanussot and P. Lambert, "Total ordering based on space filling curves for multivalued morphology," in *4th Int. Symp. on Mathematical Morphology and its Applications (ISMM '98)*, Amsterdam, The Netherlands (1998).
41. C. Song, P. Li, and F. Yang, "Multivariate texture measured by local binary pattern for multispectral image classification," in *Int. Geoscience and Remote Sensing Symp. (IGARSS'06)*, Denver, Colorado, pp. 2145–2148 (2006).
42. A. Porebski, N. Vandenbroucke, and L. Macaire, "Haralick feature extraction from LBP images for color texture classification," in *Proc. of the Int. Workshops on Image Processing Theory, Tools and Applications (IPTA'08)*, Sousse, Tunisie, pp. 1–8 (2008).
43. T. Ojala et al., "Outex–New framework for empirical evaluation of texture analysis algorithms," in *Proc. of the 16th Int. Conf. on Pattern Recognition (ICPR'02)*, Vol. **1**, pp. 701–706, IEEE Computer Society, Québec City, Canada (2002)., http://www.outex.oulu.fi/index.php?page=classification
44. F. Bianconi and A. Fernández, "An appendix to 'texture databases—a comprehensive survey'," *Pattern Recognit. Lett.* **45**, 33–38 (2014).
45. T. Ojala, M. Pietikäinen, and T. Mäenpää, "Multiresolution gray-scale and rotation invariant texture classification with local binary patterns," *IEEE Trans. Pattern Anal. Mach. Intell.* **24**, 971–987 (2002).
46. R. Lakmann, "Barktex database of color texture images," ftp://ftphost.uni-koblenz.de/outgoing/vision/Lakmann/BarkTex (1998).
47. A. Porebski et al., "A new benchmark image test suite for evaluating color texture classification schemes," *Multimedia Tools Appl.* **70**, 543–556 (2014)., https://www-lisic.univ-littoral.fr/~porebski/BarkTex_image_test_suite.html

48. M. Lecca, "On the von Kries model: estimation, dependence on light and device, and applications," in *Advances in Low-Level Color Image Processing*, Vol. **11**, Lecture Notes in Computational Vision and Biomechanics, Chapter 4, pp. 95–135, Springer, Netherlands (2014).
49. A. Ledoux, O. Losson, and L. Macaire, "ALOT texture classification dataset," 2015, http://lagis-vi.univ-lille1.fr/datasets/alot.html
50. C. Cusano, P. Napoletano, and R. Schettini, "Evaluating color texture descriptors under large variations of controlled lighting conditions," *J. Opt. Soc. Am. A* **33**, 17–30 (2016).
51. K. Hammouche, O. Losson, and L. Macaire, "Extended outex texture classification test suites," 2015, http://lagis-vi.univ-lille1.fr/datasets/outex.html
52. L. Liu et al., "Extended local binary patterns for texture classification," *Image Vision Comput.* **30**(2), 86–99 (2012).
53. M. Côté and A. B. Albu, "Robust texture classification by aggregating pixel-based LBP statistics," *IEEE Signal Process Lett.* **22**, 2102–2106 (2015).
54. J. Xie et al., "Effective texture classification by texton encoding induced statistical features," *Pattern Recognit.* **48**(2), 447–457 (2015).

Audrey Ledoux obtained her MS degree in 2010 and her PhD in image processing in 2013 from the University of Poitiers, France. She was in a postdoc position for nine months at XLIM-SIC Laboratory, University of Poitiers, and for one year in the CRIStAL Laboratory, University of Lille 1. She is presently associated with teaching and research in the CRIStAL Laboratory. Her research interests focus on color image processing, color mathematical morphology, and color texture analysis.

Olivier Losson received his MS (engineer) degree in 1994 from the École Centrale of Lille, France, and his PhD in computer science and control from the University of Lille 1 in 2000. He is an associate professor at the Department of Computer Science, Electronics, Electrical Engineering and Automatics, and a member of the CRIStAL Laboratory, University of Lille. His research interests focus on color image processing, chiefly image demosaicing, color image segmentation, and color texture representation.

Ludovic Macaire received his MS (engineer) degree in computer science from the UTC Engineering School of Compiègne, France, in 1988 and his PhD in computer science and control from the University of Lille 1 in 1992. He is presently a full professor in the CRIStAL Laboratory, University of Lille1 and in the ANR-11-EQPX-23 IrDIVE platform. His research interests include color representation, color image analysis applied to segmentation and retrieval (REPAR project funded by NordPas-de-Calais Region).